EXAMINING THE ROLE OF OIP5 AND PCSK5 EXPRESSION IN PAPILLARY RENAL CELL CARCINOMA (pRCC) TUMORIGENESIS

By:

BRYAN HUONG

Thesis Submitted to McMaster University for Partial Fulfillment of Requisite for Master of Science Degree

MASTER OF SCIENCE (2022)

Faculty of Health Sciences, Medical Sciences Graduate Program – Cancer and Genetics

McMaster University, Hamilton, Ontario, Canada

TITLE: EXAMINING THE ROLE OF OIP5 AND PCSK5 EXPRESSION IN PAPILLARY RENAL CELL CARCINOMA (pRCC) TUMORIGENESIS

AUTHOR: Bryan Huong, McMaster University

SUPERVISOR: Damu Tang

SUPERVISORY COMMITTEE: Dr. Anil Kapoor, Dr. Mark Inman

TABLE OF CONTENTS

LAY ABSTRACT 4
ABSTRACT 5
ACKNOWLEDGMENTS 7
LIST OF FIGURES 8
LIST OF ABBREVIATIONS 9
1. INTRODUCTION 11
1.1 Renal Cell Carcinoma (RCC) 11
1.2 OPA Interacting Protein 5 (OIP5) 14
1.3 OIP5 and RCC 16
1.4 Proprotein Convertase Subtilisin/Kexin Type 5 (PCSK5) 18
1.5 PCSK5 and RCC 19
2. OBJECTIVES AND HYPOTHESIS 20
3. MATERIALS AND METHODS 22
3.1 Materials 22
3.2 Methods 23
3.2.1 Tissue Culture 23
3.2.2 Subcloning 23
3.2.3 Transfection and Stable Lines 23
3.2.4 Cell Lysis and Western Blot 24
3.2.5 Colony Formation Assay 25
3.2.6 Renal Subcapsular Transplantation and Luminescent Imaging of Tumor 25
3.2.7 Organ Collection and Fixation of Xenograft Tumors 26
3.2.8 Immunohistochemistry 26
3.2.9 Real-time PCR (RT-PCR) 27
3.2.10 Statistical Analysis 27
4. RESULTS 28
4.1 OIP5 Overexpression Leads to Increased Colony Formation in ACHN 28
4.2 OIP5-derived Enhancement of pRCC Tumor Growth in an Orthotopic Tumor Model . 31
4.3 PCSK5 promoting pRCC Tumorigenesis 37

5. DISCUSSION 44
6. FUTURE DIRECTION 48
7. REFERENCES 49

LAY ABSTRACT

This project focuses on renal cell carcinoma (RCC) which is a cancer that originates from renal tubular epithelial cells in the kidneys. The elusive and vast nature of RCC leads to many subtypes that differ histologically and biologically and thus require different diagnoses and treatments. By investigating the papillary RCC (pRCC) subtype, the goal is to identify potential biomarkers for pRCC that may aid in future clinical diagnosis and treatment. OIP5 is a protein scarcely investigated and past studies have shown its overexpression linked to pRCC progression and tumorigenesis, but further metastatic investigation is warranted. This study aimed to confirm OIP5 overexpression plays a role in cancer as well as use a luciferase firefly reporter gene to monitor OIP5's role in tumorigenesis and metastatic potential *in vivo* using a live mouse model. Results suggest that OIP5 overexpression plays a role in enhanced tumor growth *in vivo*. PCSK5 is another fairly novel gene of interest in this study, and while research involving PCSK5 and RCC is severely limited, recent studies imply it may be affected by different oncogenes such as OIP5 and specific microRNA during ccRCC and pRCC progression. Therefore, this study investigated the presence of PCSK5 in OIP5 pRCC tissue and tumors. The results suggest that PCSK5 has a higher presence in OIP5 overexpressed cells and tissue as well as a higher mRNA presence. Figures created using public genomic datasets show a correlation between PCSK5 and OIP5 expression during the later stages of pRCC progression and with lower survival probabilities. This indicates the possibility of interaction between OIP5 and PCSK5 and if true, provides a potential link for finding more biomarkers for potential future therapeutic targeting.

ABSTRACT

Renal cell carcinoma (RCC) is a cancer that originates from renal tubular epithelial cells in the kidneys. Studies focusing on RCC are vital as it accounts for around 3% of all human cancers as of 2014 and accounts for over 90% of cancers affecting the kidneys. Being a heterogenous disease, RCC consists of multiple subtypes including papillary RCC (pRCC) with a 10% incidence rate. The heterogenous nature of RCC makes it difficult to determine biomarkers and therapeutic treatments that can provide adequate treatment targeting RCC in different patients, which stresses the need to discover as many therapeutic targets as possible. OIP5, also known as Mis18β, is a 25-kDa protein that is accumulated in the telophase-G1 centromere during mitosis and plays a role in centromere/kinetochore structure formation and functionality. As Mis18β, it interacts with Mis18α in a heterotetramer complex to bind and localize centromeric protein A (CENP-A) to the proper centromere region to allow for formation for centromere/kinetochore formation and function. OIP5 is normally highly expressed in the testes but recent studies have suggested that OIP5 overexpression is linked to the progression of some types of human cancers, including promoting pRCC cell proliferation and tumorigenesis. Furthermore, past studies have shown that other genes may impact RCC progression through regulation of cell growth and substrate activation extending past just the cell cycle. PCSK5 is another target of interest of focus in this study. Known also as PC6, it is a proprotein convertase which acts on precursor proteins to turn them into their active forms through post-translational modification and plays a role in cell growth and bone remodeling. This study aims to investigate the role of OIP5 during RCC progression both *in vitro* and *in vivo* with a focus on pRCC as well as investigate the expression of PCSK5 in conjunction with OIP5 and pRCC. *In vitro* studies confirmed previous results that OIP5 promotes colony formation in

ACHN pRCC cells. Using a bioluminescent reporter alongside ACHN OIP5 and ACHN empty vector (EV) cell lines, mice were injected through renal subcapsule transplantation. It was seen that, while OIP5 produced larger tumors over a wider area after 12 weeks, metastasis did not appear to occur as largely as hoped though this may be due to limitations of the model. Analysis of the ACHN xenografts showed increased expression of PCSK5 and PLK1 in the OIP5 tumors. For PLK1, this is likely due to the close nature of its function with OIP5 during mitosis while PCSK5 may be regulated by OIP5 through an unknown mechanism or through microRNA miR-101-5p. Despite this, mRNA levels of PCSK5 were insignificant between OIP5 and EV groups. pRCC patient data showing PCSK5 expression levels showed a minor correlation with OIP5 expression, as well as higher expression at later pRCC stages and leading to reduced survival probability. Overall, this thesis analyzes the relationship of OIP5 in RCC, specifically pRCC, and introduces PCSK5 as another intriguing target for further study in treating pRCC.

ACKNOWLEDGMENTS

I would like to thank my supervisor Dr. Damu Tang for giving me the opportunity these past two years as well as the last year of my undergraduate thesis program to experience and learn crucial skills required in the field of research for my future career and beyond. The lessons I have learned here will stay with me for my life and I will not forget them. The years I spent in this lab have been hard but not unrewarding. Thank you for your guidance and patience with me.

I would like to thank my committee members, Dr. Mark Inman and Dr. Anil Kapoor, for their time in attending my committee meetings and for their invaluable insight and revisions in my project throughout the years.

To my parents, thank you for encouraging me to pursue my future dreams and supporting my endeavors non-stop. Whenever things get hard and I struggle to find the right direction, I know you always love and support me in whatever I do and have faith in me to learn and find a way.

To all my friends, thank you for being my source of destress and encouragement. I cherish you all for listening to my rants and supporting me in my thoughts and problems and for the countless laughs and memories. When I felt alone and stressed in lab, I always knew I had you guys to reach out to. Thanks for keeping me sane throughout my academic career.

To my girlfriend Selena, I am so lucky to have you supporting me every single day while navigating my thesis. Thank you for holding me accountable, giving me advice, always being there whenever I need to talk, and making sure I am eating and taking care of myself. I am always grateful for your support.

LIST OF FIGURES

Figure 1. - OIP5 (Mis18β) Role in Cell Cycle 15
Figure 2. - ACHN OIP5-Luc Western Blot Analysis 28
Figure 3. - ACHN OIP5-Luc Colony Formation Assay 29
Figure 4. - ACHN OIP5-Luc *In Vivo* Bioluminescent Imaging 32
Figure 5. - ACHN OIP5-Luc Kidney Tumor Images 33
Figure 6. - ACHN OIP5-Luc IHC Analysis for OIP5 35
Figure 7. - ACHN OIP5-Luc IHC Analysis for PLK1 36
Figure 8. - ACHN OIP5-Luc IHC Analysis for PCKS5 38
Figure 9. - ACHN OIP5 Xenograft IHC Analysis for PCSK5 40
Figure 10. - Correlations between PCSK5 and OIP5 mRNA Expressions 42
Figure 11. - PCSK5 Expression in Various pRCC Stages 43
Figure 12. - pRCC Patient Survival Probability with Different PCSK5 Expressions 43

LIST OF ABBREVIATIONS

CCK-8 - Cell counting kit-8

CDK - Cyclin-dependent kinase

ccRCC - Clear cell renal cell carcinoma

CENP-A - Centromeric protein A

EV - Empty vector

FH - Fumarate hydratase

HGF - Hepatocyte growth factor

HIF - Hypoxia-inducible factor

HJURP - Holliday junction recognition protein

IHC - Immunohistochemistry

M18BP1 - Mis18-binding protein 1

MET - Mesenchymal-epithelial transition

NOD/SCID - Nonobese diabetic/severe combined immunodeficiency

OIP5 - OPA interacting protein 5

OPN - Osteopontin

PCSK5 - Proprotein convertase subtilisin/kexin type 5

PLK1 - Polo-like kinase 1

pRCC - Papillary renal cell carcinoma

RCC - Renal cell carcinoma

RT-PCR - Reverse transcription polymerase chain reaction

siRNA - Small interfering RNA

VHL - von Hippel–Lindau

1. INTRODUCTION

1.1 Renal Cell Carcinoma (RCC)

Renal cell carcinoma (RCC) originates from renal tubular epithelial cells in the kidneys. The disease accounts for around 3% of all human cancers as of 2014 and accounts for over 90% of cancers affecting the kidneys (Chow, 2020; Hsieh et al., 2017). The worldwide incidence rate is approximately 431,000 new cases and 179,000 deaths annually, with these numbers slowly increasing over several years in all stages of the cancer (WCRF International, 2022). In Canada alone, 7500 individuals are expected to be diagnosed with kidney cancer annually and 2000 are expected to die (Canadian Cancer Survivor Network, 2020). The majority of RCC cases are sporadic and only 2-3% of cases were familial (Chow, 2020). RCC is more prominent in men with approximately double the incidence rate compared to women (Hotte et al, 2019). Men have been linked to more severe and prominent RCC prognosis, though this is likely a combination of both genotypic and lifestyle factors typically associated with RCC onset as discussed further on (Mancini et al., 2020). A variety of different risk factors are linked with RCC. Lifestyle factors such as diet, obesity, smoking history, exposure to environmental pollutants, past diseases, as well as genotypic factors such as specific sex hormones and sex-specific differences in gene expression are all associated with RCC (Chow, 2020; Mancini et al., 2020).

Early RCC diagnosis relies on internal imaging using ultrasound, MRI, and CT scanning, and due to it being asymptomatic in the early stages, it is often discovered after a patient has undergone scanning for an unrelated issue (Gray & Harris, 2019). There are four stages used to classify RCC progression in the body which are related to tumor and metastatic progression (National Cancer Institute, 2022) In Stage 1, a tumor less than 7 centimeters in size forms in the

kidney and is localized to that region only. Stage 2 begins when the tumor is larger than 7 cm but is still localized in the kidney with no metastatic growth. Once metastasis has occurred and the cancer has spread beyond the kidney to the nearby lymph nodes, blood vessels, and/or the fatty tissue layer surrounding the kidney, the cancer is in Stage 3. Lastly, Stage 4 is classified by further metastatic growth where the cancer has spread beyond the kidney region to other organs such as the adrenal gland, lungs, and even the brain (National Cancer Institute, 2022).

Being a heterogenous disease, RCC consists of multiple subtypes differing histologically (Chow, 2020). The most common subtypes are clear cell RCC (ccRCC) with a 75% incidence rate and papillary RCC (pRCC) with a 10% incidence rate (Muglia & Prando, 2015). 95% of ccRCC cases were sporadic, meaning patients developed this disease without any prior hereditary factors involved. The other 5% were associated with hereditary conditions such as von Hippl-Lindau disease or tuberous sclerosis (Muglia & Prando, 2015). Histologically, ccRCC is classified by a visible cluster of cells with a clear cytoplasm and it originates from the proximal convoluted tubules epithelium (Muglia & Prando, 2015). Mutation of the *VHL* gene affecting downstream targets appears to be the main factor leading to ccRCC development (Sanchez-Gastaldo, 2017). The *VHL* gene encodes for a protein responsible for regulating the activity of hypoxia-inducible factor (HIF), a transcription factor that alters cell activity in response to variable oxygen availability (such as in hypoxic conditions) (Sanchez- Gastaldo et al., 2017). Under normoxic conditions, *VHL* promotes the ubiquitination and degradation of HIF, but a mutated *VHL* gene is unable to downregulate HIF which leads to increased cell growth and energy production, promoting RCC progression in the process (Sanchez-Gastaldo et al., 2017). Overall *VHL* acts as a tumor suppressor and its mutation is the driving factor for ccRCC initiation.

pRCC has two variations that originate in the distal nephron tubule epithelium but differ histologically and pathologically: Type 1 and Type 2 variants. Characteristics of Type 1 pRCC involve alterations in the MET pathway while Type 2 is associated with mutations in the fumarate hydratase (FH) gene associated with the Kreb's cycle (Sanchez-Gastaldo, 2017). Histologically, Type 1 can be seen as a single layer of basophilic cells around a basal membrane with visible dark nuclei while Type 2 is associated with papillae covered by cells with granular cytoplasms and large nuclei (Muglia & Prando, 2015). The MET gene encodes for a transmembrane receptor that interacts with a hepatocyte growth factor (HGF) that, when bound to its receptor, signals various cellular pathways promoting cell proliferation through a variety of second messengers (Sanchez-Gastaldo, 2017). Type 1 pRCC is associated with a mutation in MET which leads to permanent activation of the HGF receptor, in turn contributing to uncontrolled cell proliferation (Sanchez-Gastaldo, 2017). In Type 2 pRCC, mutations in the fumarate hydratase (FH) gene lead to its inactivation. FH plays a role in decreasing the intracellular levels of fumarate in the Kreb's cycle and when unregulated, fumarate accumulation prevents the degradation of HIF through hydroxylation which, as seen in ccRCC previously, promotes cell changes involving cell growth (Sanchez-Gastaldo, 2017).

As a heterogeneous disease, RCC diagnosis and treatment highly depends on the subtype being diagnosed as each of the many subtypes differ in many ways such as histologically, biologically, and behaviorally (Muglia & Prando, 2015). This makes it exceedingly difficult to determine suitable biomarkers and therapeutic treatments that can provide consistent wide-spread positive effects on treating RCC in different patients, which stresses the need to discover as many therapeutic targets as possible. According to Muglia & Prando, 2015, there has been progress in

differentiating ccRCC and other subtypes in the clinical field, but the need to discover more potential biomarkers to combat these subtypes and RCC is still great.

1.2 OPA Interacting Protein 5 (OIP5)

OIP5 is the gene of interest for this study. Also known as Mis18β, it is a 25-kDa protein that is normally highly expressed in the testes. It is specifically accumulated in the telophase-G1 centromere during mitosis and plays a role in centromere/kinetochore structure formation (Gong et al., 2013). The presence of kinetochores is essential to the proper segregation of chromosomes and subsequently, the division of cells in mitosis (Pan et al., 2019). During the mitotic phase of the cell cycle, kinetochores emerge from a chromosomal region called the centromere (Pan et al., 2019). These centromeres contain nucleosomes with the histone H3 variant centromeric protein A (CENP-A) which requires replenishing at the proper nucleosome location every cell cycle, and this is done through a chaperone complex consisting of the Holliday junction recognition protein (HJURP), a two-subunit Mis18 complex made of Mis18α and Mis18β, and Mis18-binding protein 1 (M18BP1) (Pan et al., 2019) (**Figure 1**). Mis18β interacts with these different proteins to bind and localize CENP-A to the proper centromere region where it then recruits inner kinetochore proteins CENP-C and CENP-N to fully assemble the entire kinetochore (Pan et al., 2019). The specific process involves Mis18β forming a heterotetramer with Mis18α and joining with Mis18BP1 to form a complex which then interacts with HJURP carrying CENP-A. This interaction then leads to CENP-A being directed to its proper location in the nucleosome (Pan et al., 2019) (**Figure 1**). CENP-C and CENP-N interact with CENP-A on the nucleosome throughout this process to support and stabilize its insertion and ensure CENP-A acts as a suitable epigenetic

marker for successful kinetochore assembly (Pentakota et al., 2017). This overall process occurs every cell replication cycle. Other factors positively and negatively regulate this process. Polo-like kinase 1 (PLK1) interacts with Mis18β to stabilize the protein and the Mis18 heterotetramer complex (McKinley, Cheeseman, 2015) (**Figure 1**). Cyclin-dependent kinases 1/2 (CDK1/2) phosphorylate HJURP to prevent binding to the Mis18 complex and therefore CENP-A localization (**Figure 1**).

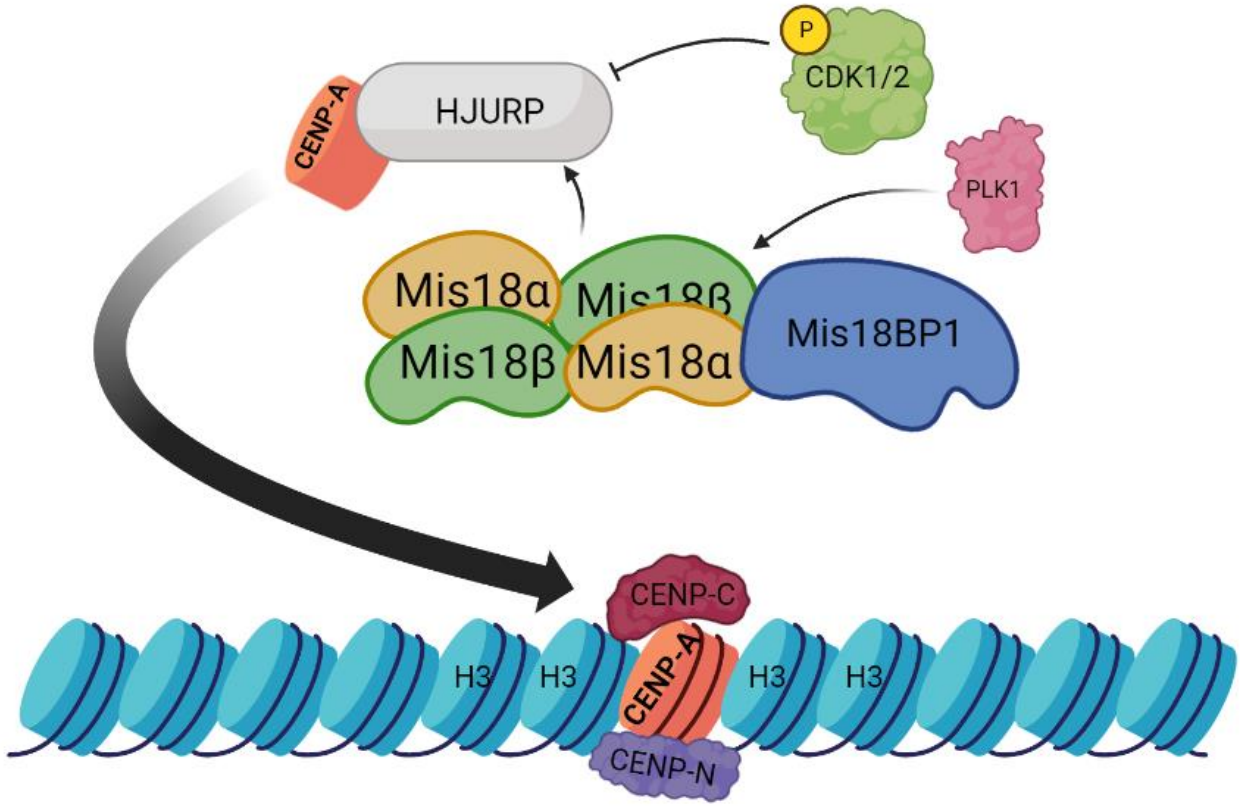

Figure 1. Diagram illustrating role of OIP5 (Mis18β) in centromere function. OIP5 forms heterotetramer with Mis18α and then binds with Mis18BP1 to make up Mis18 complex. This complex interacts with HJURP carrying CENP-A to be localized to the nucleosome, replace a histone H3. PLK1 positively regulates CENP-A localization by binding to and stabilizing OIP5. CDK1/2 negatively regulates CENP-A localization by phosphorylating HJURP. CENP-C and CENP-N bind to CENP-A on nucleosome to stabilize and assemble kinetochore structure.

1.3 OIP5 and RCC

It had been suggested previously that OIP5 overexpression is linked to the progression of several types of human cancers including kidney, lung, and bladder cancers (Gong et al., 2013; Li et al., 2019). OIP5 interacts with different oncogenic proteins from major pathways including Raf1 and Akt (Li et al., 2017). Raf1 is part of the MAPK/ERK signaling pathway which plays a major role in cell signaling response, and it was found that the signaling pathway is involved in resistance to chemotherapy (Li et al., 2016). Raf1 expression was found to be involved in tumor growth and metastasis, and the cell signaling responses initiated by it promote tumor cell survivability (Hatzivassiliou et al., 2003; Koinuma et al., 2012). With regards to OIP5, it was found that Raf1 expression regulates OIP5 stability in lung cancer as well as protein levels of OIP5 (Koinuma et al., 2012). With Akt, it was found that OIP5 increased Akt phosphorylation in liver cancer (Li et al., 2017). The Akt signaling pathway is a major player involved in cell survival, and by facilitating Akt phosphorylation, OIP5 triggers tumor growth through mTORC2 while inhibiting p38 activity which would inhibit Akt signaling (Brito et al., 2015; Hua et al., 2017). Despite this, there is still a lack of reported studies investigating the biological function of OIP5 expression on RCC activity. An RT-PCR analysis done on ccRCC tissue and neighboring non-tumor tissue demonstrated that mRNA levels of OIP5 were elevated in ccRCC tissues (Gong et al., 2013). Gong et al. (2013) then plotted survival curves to determine the 5-year cumulative survival rate of ccRCC patients with varying levels of OIP5 expression. Their results showed that patients with high expression had a significantly lower survival rate (53.2%) compared to the low expression group (81.2%), suggesting that OIP5 overexpression could be a biomarker for predicting the severity of ccRCC progression in patients. In addition, experiments utilizing small interfering RNA (siRNA) to target

and knock down OIP5 expression in 786-O and Caki-2 cell lines alongside colony formation assay and Cell Counting Kit-8 (CCK-8) demonstrated that reduced OIP5 expression also led to reduced cell growth in the OIP5 siRNA cell lines compared to the control group cell lines (Gong et al., 2013). Recent experiments done in our lab on analyzing OIP5 expression in pRCC appear to be the first of their kind to be reported. These various experiments using the human ACHN (pRCC) cell line were done to investigate the effects of OIP5 overexpression specifically in pRCC cell proliferation. A cell proliferation assay comparing the ACHN OIP5-transfected cell line with an ACHN empty vector (EV) control group demonstrated that after 2 weeks, the number of ACHN OIP5 cells were significantly higher than the ACHN EV group (Chow, 2020). To follow up, a colony formation assay was done with the same two groups. Results showed that, relative to the number of cells seeded, the ACHN OIP5 cells showed a 2-fold increase in colonies formed compared to the ACHN EV cells (Chow, 2020). The same results were demonstrated in a transwell invasion assay using the same groups, with a higher percentage of ACHN OIP5 cells passed through the membrane after 24 hours (Chow, 2020). Alongside these results, experiments were done *in vivo* to visualize OIP5's involvement in tumor progression and mice survival. Mice bearing ACHN OIP5 and ACHN EV xenografts were compared to determine their time to endpoint (days) as a measure of survival time as well as tumor volume up until endpoint. The results showed that the ACHN OIP5 mice reached endpoint significantly sooner than their ACHN EV counterparts (Chow, 2020). Overall, these results demonstrate that OIP5 expression plays an active role in cell proliferation and tumor growth in ccRCC and pRCC. Lastly, Chow (2020) reports that Polo-like kinase 1 (PLK1) plays an important role throughout mitosis relating to kinetochore function and works in the same phase as OIP5. PLK1 aids in the localization of CENP-A by interacting with the Mis18 complex during G1. Therefore, interactions involving PLK1 and its related pathways

may be an important part to understanding OIP5's behaviour in pRCC. Further studies with OIP5 are warranted.

1.4 Proprotein Convertase Subtilisin/Kexin Type 5 (PCSK5)

OIP5's oncogenic actions rely on its interaction with multiple factors; evidence suggests PCSK5 being one of these factors (Chow et al., 2021). Upregulation of PCSK5 was observed in xenografts produced by ACHN OIP5 cells compared to ACHN EV cells (Chow et al., 2021). Therefore, PCSK5 is another target of interest of focus in this study. Known also as PC6, it is a proprotein convertase which acts on precursor proteins to turn them into their active forms through post-translational modification (Cao et al., 2001). It does this by selective cleavage of the precursor polypeptide at specific sites near single or paired basic amino acids (Cao et al., 2001). In mammals, PCSK5 is part of the family of proteins including PCSK1, PCSK2, PCSK4, and others (Seidah, Chretien, 1999). PCSK5 and its related proteins target substrates that range from inactive growth factors to cell surface receptors and glycoproteins though each member of the family has a specific tissue distribution where they act on tissue-specific substrates (Hoac et al., 2018). PCSK5 has two variants, PC5A and PC5B, which are expressed in many mice tissue including bone and tooth (Hoac et al., 2018). PCSK5 was reported to facilitate the function of osteopontin (OPN), a highly abundant extracellular matrix protein which plays a role in cell adhesion, signaling, and bone modelling and growth in mice (Hoac et al., 2018). OPN cleavage by PCSK5 could affect the binding properties of the matrix protein and thus lead to changes in bone cell migration and bone development (Hoac et al., 2018). Overall, PCSK5's potential involvement in different cell and

tissue behaviours through post-translational modification of precursor proteins makes it an interesting target to study.

1.5 PCSK5 and RCC

While not much research has been done yet with regards to PCSK5 and its role in RCC, there have been several studies that imply its involvement in the progression of different RCC subtypes. It was found that PCSK5 is a potential oncogene in ccRCC due to it being one of many genes controlled by microRNA miR-101-5p, whose upregulation correlates with cell cycle arrest and apoptosis (Yamada et al., 2020). Furthermore, studies have shown evidence that PCSK5 may be affected by different oncogenes with regards to pRCC progression. In a study investigating differentially expressed genes with regards to ACHN OIP5 and ACHN EV pRCC tumors, it was found that PCSK5 was one of several genes with a significant difference in expression between groups as well as further elevation in Stage 3 and 4 pRCC tumors (Chow et al., 2021). Therefore, further analysis on PCSK5 expression is warranted.

2. OBJECTIVES AND HYPOTHESIS

While past studies have demonstrated an association between OIP5 and different types of cancer, and more recent studies focusing on its involvement in RCC, there is still a lack of experimental reports investigating the biological link between OIP5 and RCC in the scientific field. The limited results reported have shown OIP5 overexpression linked to poor prognosis and survival rate as well as greater cell proliferation and tumor growth (Gong et al., 2013; Chow et al., 2021). As of writing, no studies have yet been reported that involve monitoring OIP5 expression in relation to RCC metastatic growth potential *in vivo* through imaging means such as bioluminescence. Past studies have shown that a renal subcapsular transplantation approach was seen to have better success in promoting metastasis in live mice models compared to subcutaneous injection which justifies the *in vivo* approach taken in this study.

Another target gene of interest is PCSK5, a proprotein convertase that has shown to be potentially upregulated in pRCC tumors. With limited data regarding PCSK5 and its link to RCC progression, investigating its expression in ACHN cell-produced tumors with regards to OIP5 overexpression can provide valuable insight on PCSK5's potential interaction in the cell cycle and act as a steppingstone for identifying PCSK5's target substrates. This could allow for the discovery of an underlying involvement that PCSK5 may have on cell proliferation.

The objectives of this study are to build upon past experiments investigating the role of OIP5 during RCC progression both *in vitro* and *in vivo* with a focus on pRCC as well as investigate the expression of PCSK5 in conjunction with OIP5 and pRCC. Also, with a potential reliance on PLK1 for OIP5 functional stability reported by Chow (2020), it would be interesting to briefly

investigate PLK1 presence in OIP5-overexpressed tissue to confirm the connection between the two. This study involves the following:

- Using a bioluminescence-tagged plasmid incorporated into ACHN OIP5 and ACHN EV cell lines and xenografts to monitor renal subcapsular tumor growth and metastasis *in vivo.*
- Obtaining ACHN OIP5 and ACHN EV xenografts, IHC and RNA studies can be performed to examine the expression of PCSK5 and PLK1, both of which potentially play a role in pRCC properties and progression.

It is hypothesized that OIP5 overexpression will contribute to improved RCC metastatic growth potential *in vivo* and that PCSK5 and PLK1 expression will be upregulated in ACHN OIP5 tumors compared to ACHN EV tumors, owing to their change in expression and close role with OIP5 as pRCC progresses.

3. MATERIALS AND METHODS

3.1 Materials

Aprotonin, leupeptin, calcium chloride ($CaCl_2$), ethanol, crystal violet dimethyl sulfoxide (DMSO), phenylmethysulfonyl fluoride (PMSF), ammonium persulphate (APS), β-mecaptoethanol, EDTA, potassium acetate, and OIP5 antibody were purchased from Sigma Aldrich. TEMED, Tris, agarose, bovine serum albumin (BSA), glycine, sodium dodecyl sulphate (SDS), sodium chloride (NaCl), sodium citrate, hydrogen chloride (HCl) were purchased from Bioshop Canada. 30% acrylamide solution was purchased from Bio-rad Laboratories. Trypsin-EDTA, Penicillin-Streptomycin, and Superscript were purchased from Invitrogen. Fetal bovine serum was purchased from Life Technologies. Methanol, xylene, and isopropyl alcohol were purchased from Caledon Laboratories. TRIzol, and SYBR Green were purchased from Fisher Scientific. DAB and ABC were purchased from Vector Laboratories. Mini plasmid kit was purchased from Geneaid. Gel extraction kit was purchased from QIAGEN. DNA ligase was purchased through New England BioLabs. Some OIP5 and PCSK5 antibodies were purchased from Proteintech. pBV-Luc and pLNCX2 plasmids were obtained from Addgene. ACHN OIP5 and EV stable lines were obtained by M. Chow. Buprenorphine painkiller, sutures, and surgical supplies were obtained through McMaster University. RT-PCR primers were obtained through Integrated DNA Technologies. D-Luciferin Potassium Salt was obtained through Goldbio and PerkinElmer.

3.2 Methods

3.2.1 Tissue Culture

ACHN OIP5 and EV cells were cultured in MEM media containing 1% Penicillin-Streptomycin and 10% fetal bovine serum. Cells were cultured at 37℃ in 50% CO_2 and 95% air with humidity. ACHN OIP5 acts as the pRCC positive model in this study and ACHN EV acts as a negative control model.

3.2.2 Subcloning

A Luc gene insert was created by splicing the pBV-Luc plasmid using restriction enzymes HindIII and SalI. pLNCX2 plasmid was spliced using HindIII and SalI at a portion of the multiple cloning site to allow for Luc to be inserted. Gel purification for the Luc insert and pLNCX2 backbone were then carried out. Afterwards, Luc was inserted into the pLNCX2 backbone using DNA ligase and positive clones were detected through agarose gel electrophoresis. Once positive clones were confirmed, transformation and purification were done to create more copies of the plasmid.

3.2.3 Transfection and Stable Lines

293T cells were transfected by Luc-pLNCX2 alongside gag-pol and VSVG plasmids in DMEM media. The media was replaced 10 hours after transfection. 24 hours after, the 293T DMEM media containing retrovirus was filtered through a 0.45μm filter using syringe and

centrifuged at 20000 rpm for 90 minutes at 4℃ to concentrate the retrovirus. The DMEM was aspirated, and the concentrated retrovirus was re-suspended in fresh MEM media. ACHN OIP5 and ACHN EV cell lines were infected by the retroviral MEM and incubated for 1 hour. Afterwards, the retroviral medium was aspirated, and fresh MEM was added. Cells were incubated for 24 hours to recover and then selected using G418 antibiotic. Surviving ACHN OIP5 and EV colonies containing stably transfected Luc-pLNCX2 were cultured. Positive expression of luciferase was confirmed using D-Luciferin potassium salt substrate and testing a portion of the cells using both a luminometer and a molecular bioluminescent imaging assay. Overall, ACHN OIP5-Luc and ACHN EV-Luc stable lines were produced in this process.

3.2.4 Cell Lysis and Western Blot

Cell lysis buffer [50mM Tris-HCl (pH 7.4- 7.5), 5mM EDTA, 150Mm NaCl, 1% Triton X-100, 1mM NaF, 10% Glycerol, 1mM β-glycerophophate, 1mM PMSF, 100μM Sodium orthovanadate (Na3VO4), 2μg/mL leupeptin, and 10μg/mL aprotinin] was used to lyse ACHN OIP5-Luc and ACHN EV-Luc cells. Protein concentration was obtained, and 50μg protein samples were prepared with 5x PSB. Samples were prepared by denaturing the protein at 100°C for 10 mins and then loaded on a 12.5% SDS-PAGE gel for electrophoresis. The contents of the gel were then transferred onto a nitrocellulose membrane. Afterwards, the membranes were blocked using 5% skim milk at room temperature for 2 hours, followed by the addition of 1:1000 OIP5 primary antibody and then shaken at 4°C overnight. The following day, anti-rabbit secondary antibody was prepared (1:2000) in 5% milk and poured over the membrane and then shaken for 1 hour at room temperature. The membranes were then washed and taken to a film development room and ECL

detection was done using X-ray film to detect protein expression. This confirmed that overexpression of OIP5 in ACHN OIP5-Luc was still present after transfection.

3.2.5 Colony Formation Assay

For the colony formation procedure, ACHN OIP5-Luc and ACHN EV-Luc cells were seeded in a 6-well plate with each cell line containing a well of 1000, 5000, and 10000 cells. After 5 days of incubation at 37°C, colonies in each well were fixed using 2% formaldehyde and stained with 0.5% crystal violet. Colony numbers and staining intensity were determined using ImageScope and H-score calculation (refer to 3.2.8 for formula).

3.2.6 Renal Subcapsular Transplantation and Luminescent Imaging of Tumor

ACHN OIP5-Luc and ACHN EV-Luc were counted and suspended in 1x PBS solution for a concentration of 8×10^4 cells/µL. Renal subcapsular transplantation surgery was done on 6-weeks-old immunodeficient NOD/SCID male mice to inject 50µL of cells (4×10^6 cells) into the left kidney subcapsule. This was done for 6 mice total (3 mice per cell line). Buprenorphine painkiller was administered pre- and post-surgery as well as the following day. The mice were carefully monitored for one week post-surgery for any complications. Starting at 7 weeks post-surgery, no visible tumor could be measured from the outside, so the mice were injected with D-Luciferin (150mg Luciferin/kg mouse weight) in PBS solution intra-peritoneally. After 15 mins the mice were taken to the Bruker X-ray Imaging machine room, anaesthetized, and placed in the X-ray chamber. Bioluminescent imaging of the tumor as well as X-ray imaging of each mouse

were taken. This procedure was done once a week until all mice had reached endpoint at week 10. Some mice had reached endpoint during week 9 and therefore have less images acquired in the results.

3.2.7 Organ Collection and Fixation of Xenograft Tumors

Once each mouse had reached endpoint and were euthanized, visible tumors near the kidney, along with the heart, lungs, liver, spleen, and left and right kidneys, were collected and fixed with 10% formalin. The formalin-fixed tissues were then processed by the Department of Histology at St. Joseph's Healthcare Hamilton. Afterwards, the tissues were embedded in paraffin.

3.2.8 Immunohistochemistry

Paraffin tissue slides for ACHN OIP5, ACHN OIP-Luc, ACHN EV, and ACHN EV-Luc tumors were cut serially using microtome and de-paraffinized in 100% xylene, 100% ethanol, and 70% ethanol. The slides were steamed in antigen retrieval buffer for 30 mins. Afterwards, a blocking step using 1% BSA and 10% normal goat serum was performed on all slides. OIP5 (1:50), PCSK5 (1:500), and PLK1 (1:300) primary antibodies were added and the slides were incubated at 4°C overnight. The following day, anti-rabbit secondary antibodies with a concentration of 1:200 were added to all slides along with ABC and DAB solution. Hematoxylin counterstaining was applied for 30 seconds and then images were taken and visualized using ImageScope software. The staining intensity of all slides was calculated into a H-score value that takes into account background signal. This was done by using the formula [H-score = (%weak positive) +

2×(%positive) + 3×(%strong positive)] to calculate the H-score of the positive stain region, and then using the same formula to calculate the background region of the tissue, and finally subtracting [Final H-score = (H-score (positive stain)) - (H-score (background)]. Statistical analysis was performed by running a student t-test, and a P-value of <0.05 was considered statistically significant.

3.2.9 Real-time PCR (RT-PCR)

RNA extraction was done on ACHN OIP5 and ACHN EV tumor tissues following the RNA extraction and RT-PCR protocol. RNA was isolated using TRIzol reagent and reverse transcription was done using Superscript IV. Quantitative RT-PCR was performed using SYBR-green and through the ABI7500 Fast Real-Time PCR System. A PCSK5 primer obtained from within Tang lab allowed for quantification of PCSK5 RNA expression in ACHN OIP5 and ACHN EV xenograft tumors.

3.2.10 Statistical Analysis

In this study, student t-test was performed for statistical analysis of experiments with two groups. A P-value of <0.05 was considered statistically significant for the results. Graphical data is present as mean + standard error (SE). Standard error was calculated by the following equation: $\frac{\sigma}{\sqrt{n}}$, where σ is the standard deviation of the samples in a group, and n is the sample size.

4. RESULTS

4.1 OIP5 Overexpression Leads to Increased Colony Formation in ACHN

Once both ACHN OIP5 and ACHN EV cell lines were stably transfected with the Luc-pLNCX2 plasmid, Western blot was performed to confirm that OIP5 was still stably overexpressed in the ACHN OIP5-Luc cell line. A difference in OIP5 expression can be seen through Western blotting using an anti-OIP5 rabbit primary antibody (1:1000) (**Figure 2**).

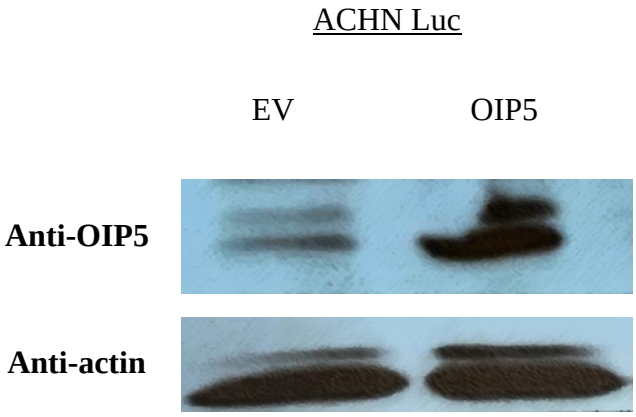

Figure 2. Western Blot analysis result showing stable overexpression of OIP5 in ACHN cell lines post-transfection with Luciferase reporter plasmid. 1:1000 Anti-OIP5 and 1:3000 Anti-actin antibodies (loading control) were used.

In addition to western blot, colony formation assay was done on ACHN OIP5 Luc and ACHN EV Luc stable lines to monitor the impact of OIP5 overexpression on colony formation (**Figure 3**).

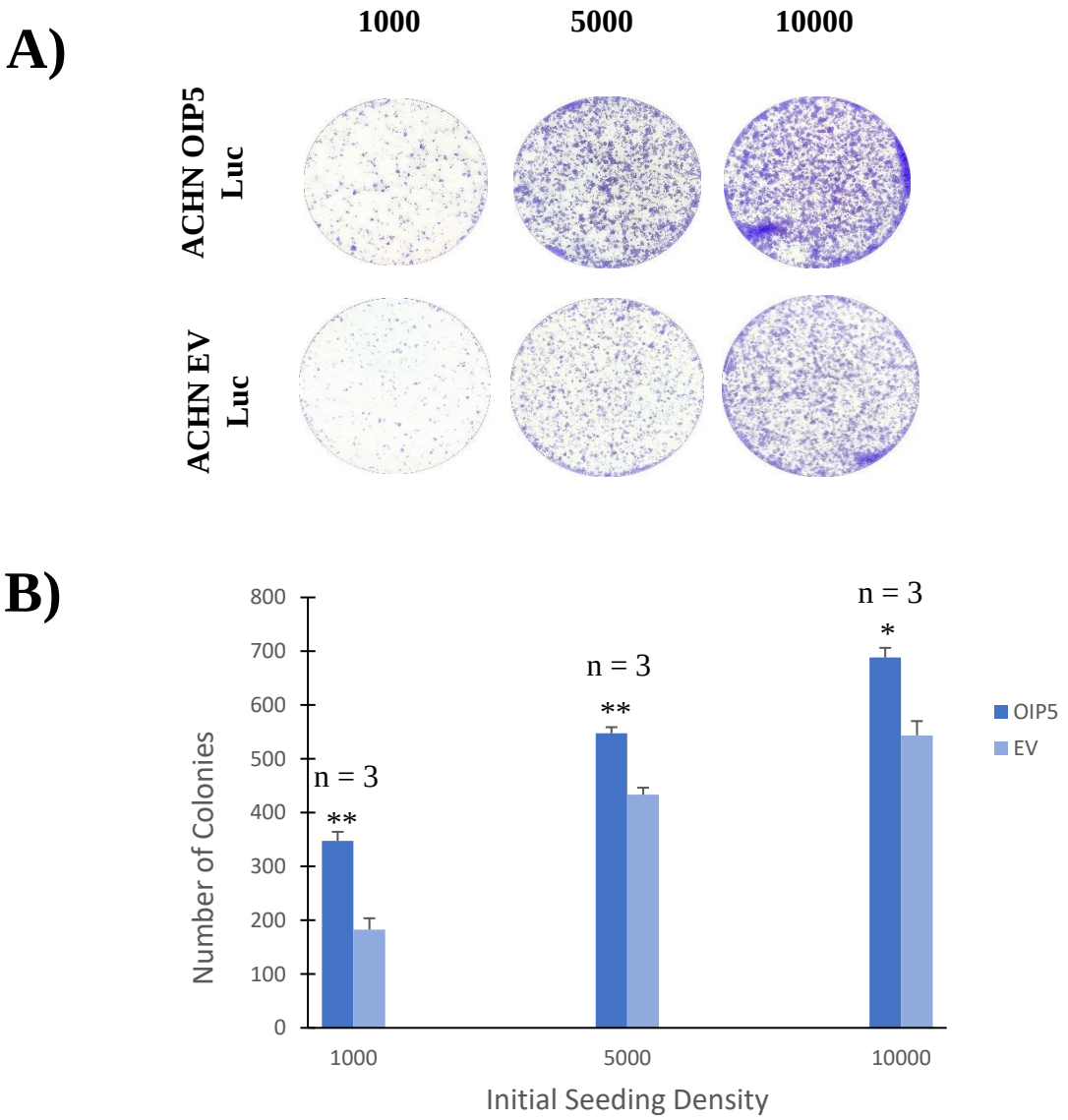

Figure 3. Colony formation assay for ACHN OIP5-Luc and ACHN EV-Luc cell lines. **A)** 6-well setup of cells showing different seeding densities and colonies formed after incubation for 5 days. **B)** Graph showing number of colonies counted after 5 days for each seeding density per group. Experiment was repeated three times (n = 3). Data shown is mean + SE. Student t-test was done as analysis. * indicates a significant difference between groups. * indicates $p \leq 0.05$, ** indicates $p \leq 0.01$.

In each of the different seeding densities used, ACHN OIP5 Luc cells formed significantly more colonies than the ACHN EV Luc cells (**Figure 3**). The average number of colonies generated for ACHN OIP5 Luc was 348 ± 17, 547 ± 11, and 688 ± 18 colonies for 1000, 5000, and 10000 seeding densities, respectively. For ACHN EV Luc, the average number was 183 ± 21, 433 ± 13, and 544 ± 27 colonies for 1000, 5000, and 10000 seeding densities, respectively. These overall observations are similar to results obtained by Chow (2020), where the OIP5-overexpressed group showed higher colony formation compared to the EV group.

4.2 OIP5-derived Enhancement of pRCC Tumor Growth in an Orthotopic Tumor Model

To further examine OIP5's oncogenic actions, we analyzed the growth/development of tumors produced by ACHN OIP5 Luc or ACHN EV Luc cells in the renal capsule space, an orthotopic RCC model. Renal subcapsular transplantation of ACHN OIP5 Luc and ACHN EV Luc stable lines was done on 12 NOD/SCID immunocompromised mice (6 per stable line). Due to surgical complications as well as lack of signal detection in some mice, images could only be collected from 6 mice (3 per stable line). Some mice had reached endpoint before week 10 and therefore only have three weeks of images. 2D area of the tumor was calculated in units of square mm using Bruker Molecular Imaging software (**Figure 4**).

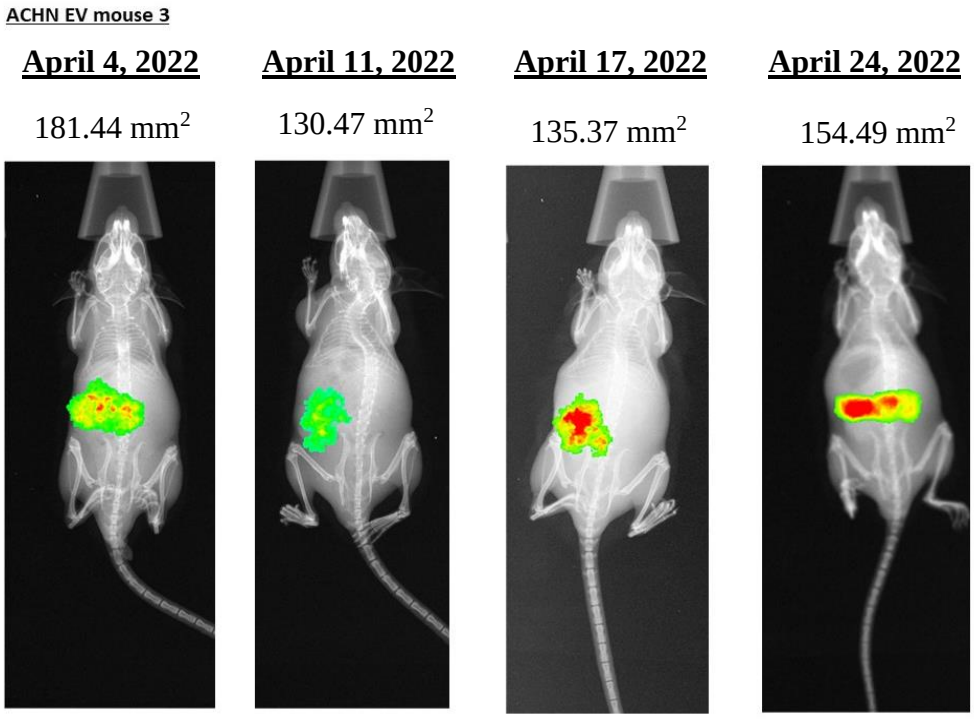

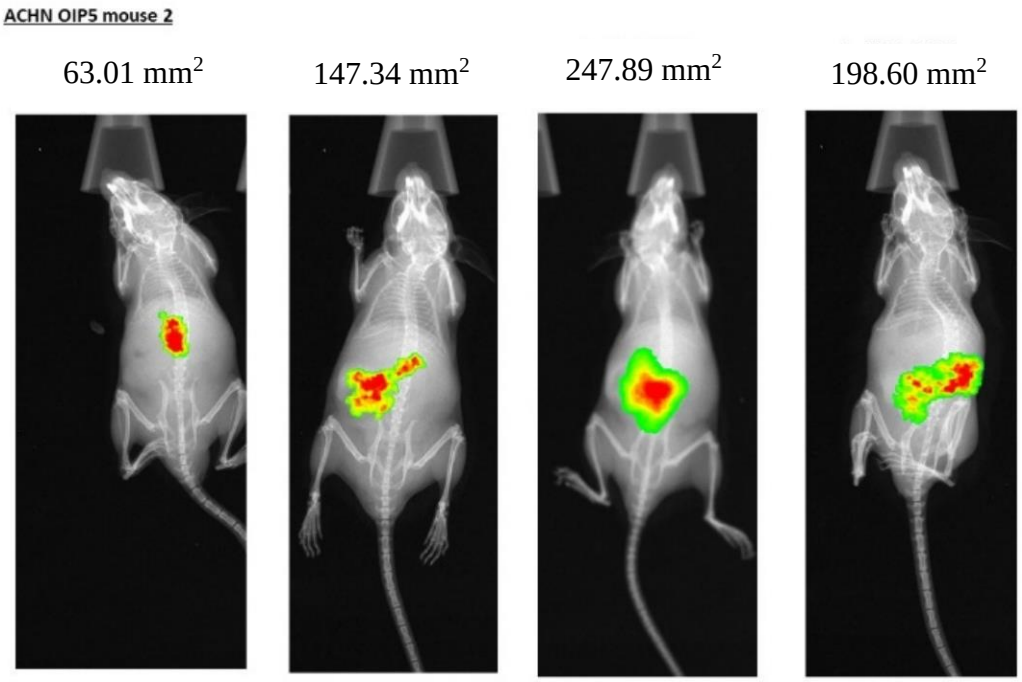

Figure 4. Representative images of one ACHN EV Luc and one ACHN OIP Luc mice and their bioluminescent/X-ray images taken from weeks 7 to 10. Tumor 2D area can be seen at the top of each image in units of square millimeters and was calculated by considering 2D regional size of the signal as well as regions of high signal intensity (red) while attempting to minimize areas of weak signal (green) which may indicate background reflective light.

Results from the bioluminescent images of the mice and the 2D tumor volumes in sq mm appear to show that tumor size is greater in mice injected with ACHN OIP5 Luc and that the tumors appear more likely to spread to different surrounding regions near the spine when compared side by side with ACHN EV Luc images (**Figure 4**). Tumor volume size is variable and does not generally show an increasing trend per mice as the weeks progress but this can be explained due to altering dynamics concerning live mice growth between weeks, what specific cells/regions the luciferin reaches in the body each injection as well as limitations pertaining to the 2D tumor calculation of the Bruker software itself and being unable to differentiate primary signal source

(tumor) from background light (reflective light). Despite this, qualitatively analyzing the 2D images themselves and the actual tumors taken from organ collection from each mice show that all three OIP5 mice grew noticeably larger tumors compared to the tumors produced in all three EV mice (see typical images in **Figure 5)**. Overall, the trend based on the bioluminescent signal and the 2D tumor volume size shows that ACHN OIP5 Luc mice have a greater tumor size compared to ACHN EV Luc mice over the same weeks and also greater pRCC metastatic potential.

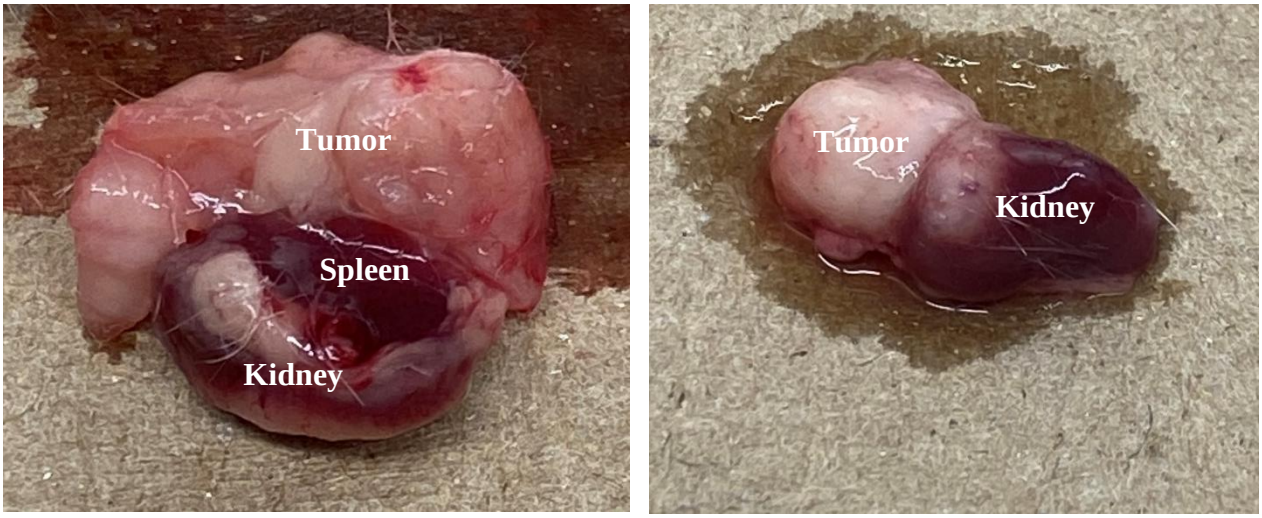

ACHN OIP5-Luc ACHN EV-Luc

Figure 5. Images of the tumor surrounding the kidney/spleen in one representative ACHN OIP5-Luc mouse and one representative ACHN EV-Luc mouse.

We further confirmed elevated OIP5 expression in xenografts produced by ACHN OIP5-Luc tumors. This was accomplished by IHC staining of ACHN EV-Luc and ACHN OIP5-Luc tumors following their collection using anti-OIP5 antibody (**Figure 6**). The average staining intensity of anti-OIP5 was 123.9 ± 4.8 for ACHN OIP5-Luc and 71.2 ± 5.5 for ACHN EV-Luc ($p<0.05$) (**Figure 6A**). Upregulation of PLK1 at the protein level in ACHN-OIP5 Luc tumors was also observed (**Figure 7**), consistent with our previous observations for a functional upregulation of PLK1 gene expression (mRNA) to OIP5-derived oncogenesis (Chow et al., 2021).

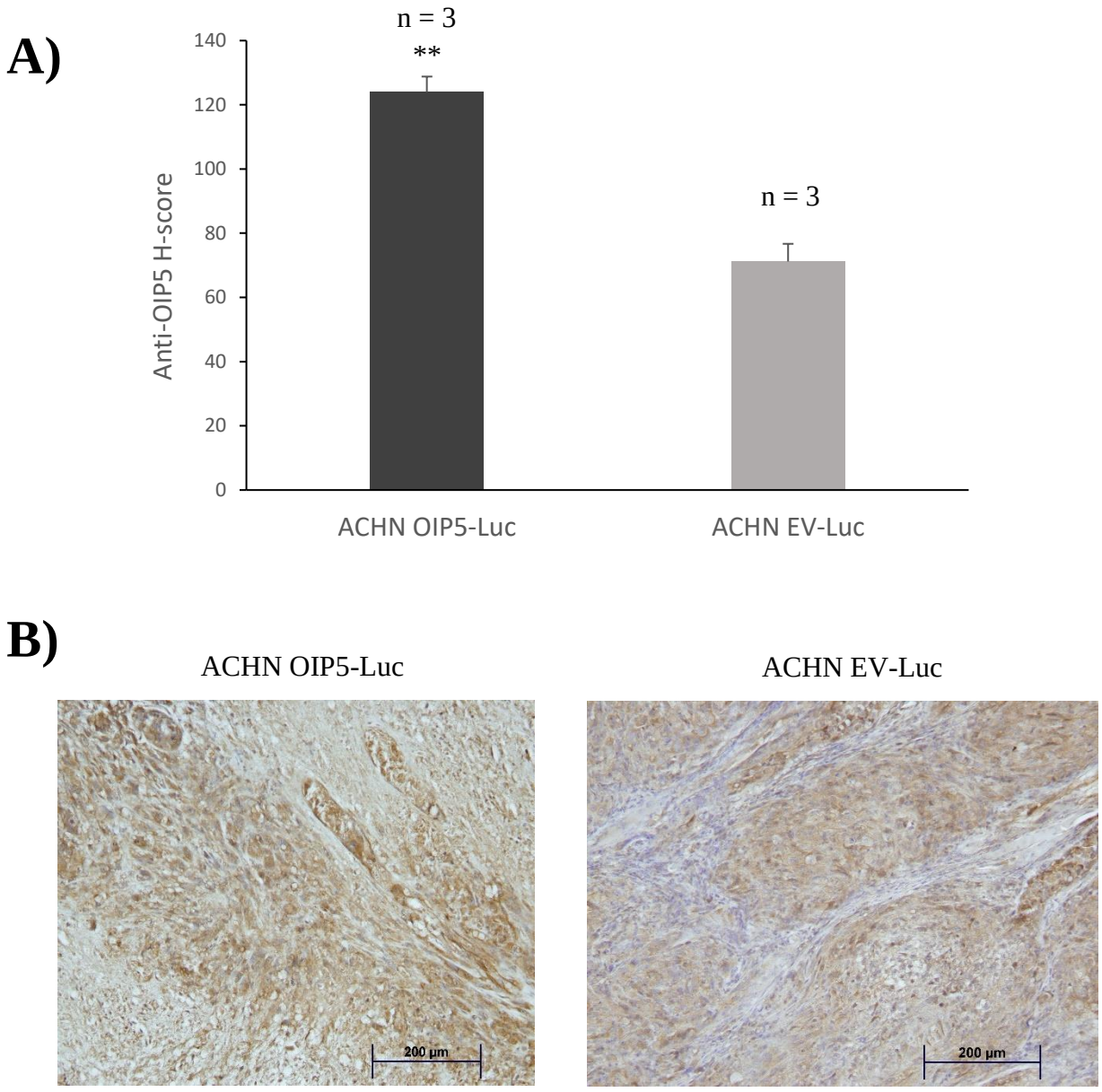

Figure 6. IHC staining and statistical analysis of OIP5 expression in ACHN OIP5-Luc and ACHN EV-Luc xenograft tumors. **A)** Graph depicting H-score of ACHN OIP5-Luc and ACHN EV-Luc xenograft tumors after staining with anti-OIP5. Experiment was repeated 3 times (n = 3). Student t-test was used to statistically analyze the results. Data shown is mean + SE. * indicates a significant difference between groups. * indicates $p \leq 0.05$, ** indicates $p \leq 0.01$. **B)** Images of anti-OIP5 IHC staining for ACHN OIP5-Luc and ACHN EV-Luc xenograft tumors.

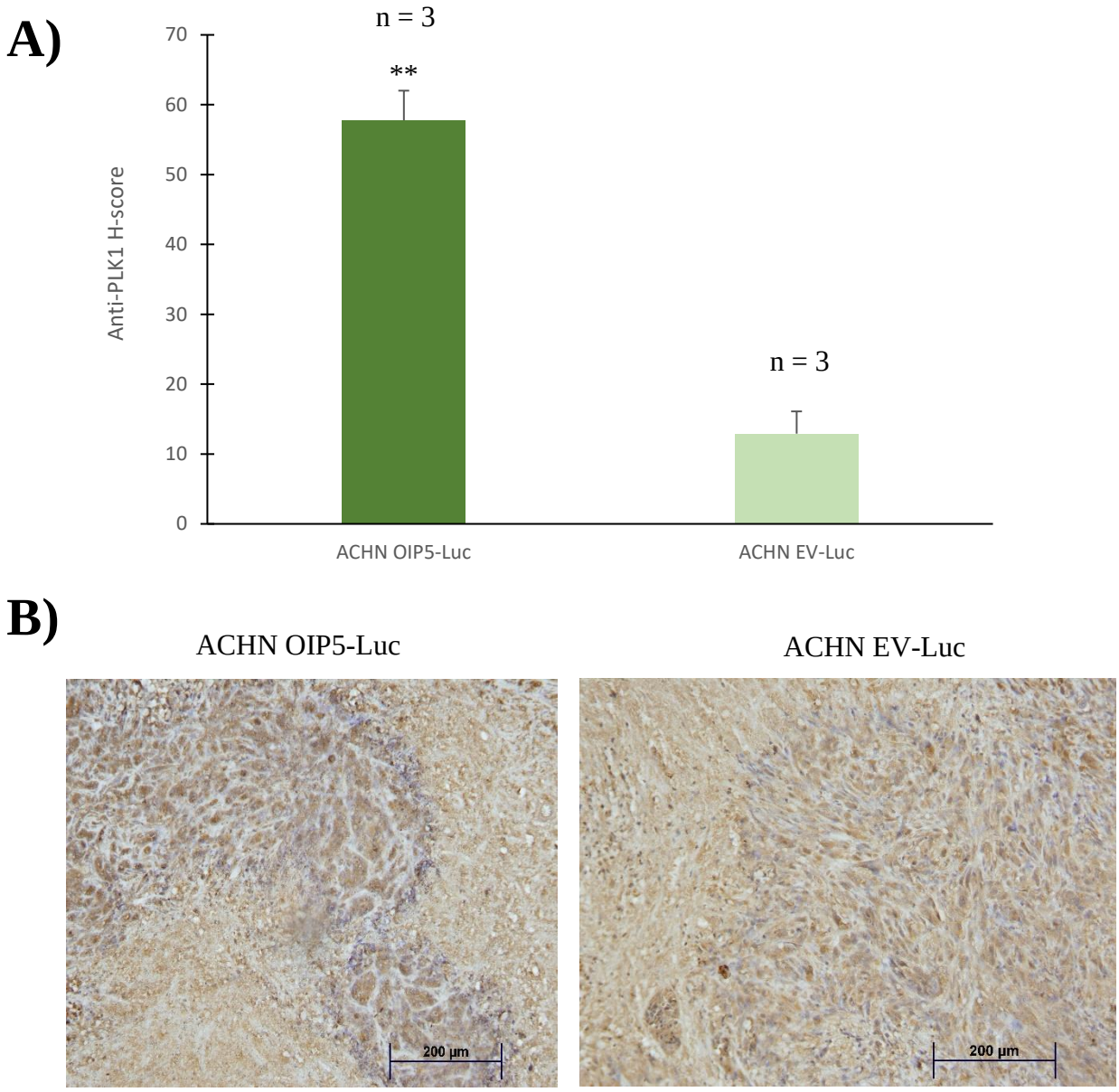

Figure 7. IHC staining and statistical analysis of PLK1 expression in ACHN OIP5-Luc and ACHN EV-Luc xenograft tumors. **A)** Graph depicting H-score of ACHN OIP5-Luc and ACHN EV-Luc xenograft tumors after staining with anti-PLK1. Experiment was repeated 3 times (n = 3). Student t-test was used to statistically analyze the results. Data shown is mean + SE. * indicates a significant difference between groups. * indicates $p \leq 0.05$, ** indicates $p \leq 0.01$. **B)** Images of anti-PLK1 IHC staining for ACHN OIP5-Luc and ACHN EV-Luc xenograft tumors.

4.3 PCSK5 associated with pRCC Tumorigenesis

Previous research from our lab revealed PCSK5 regulation by OIP5 at mRNA level (Chow et al., 2021). To study whether this upregulation also occurs at the protein level, an IHC examination for PCSK5 was performed on ACHN EV-Luc and ACHN OIP5-Luc tumors produced in the orthotopic pRCC tumor model. Results show a significant increase of PCSK5 in ACHN OIP5-Luc tumors compared to ACHN OIP5-EV tumor (**Figure 8)**.

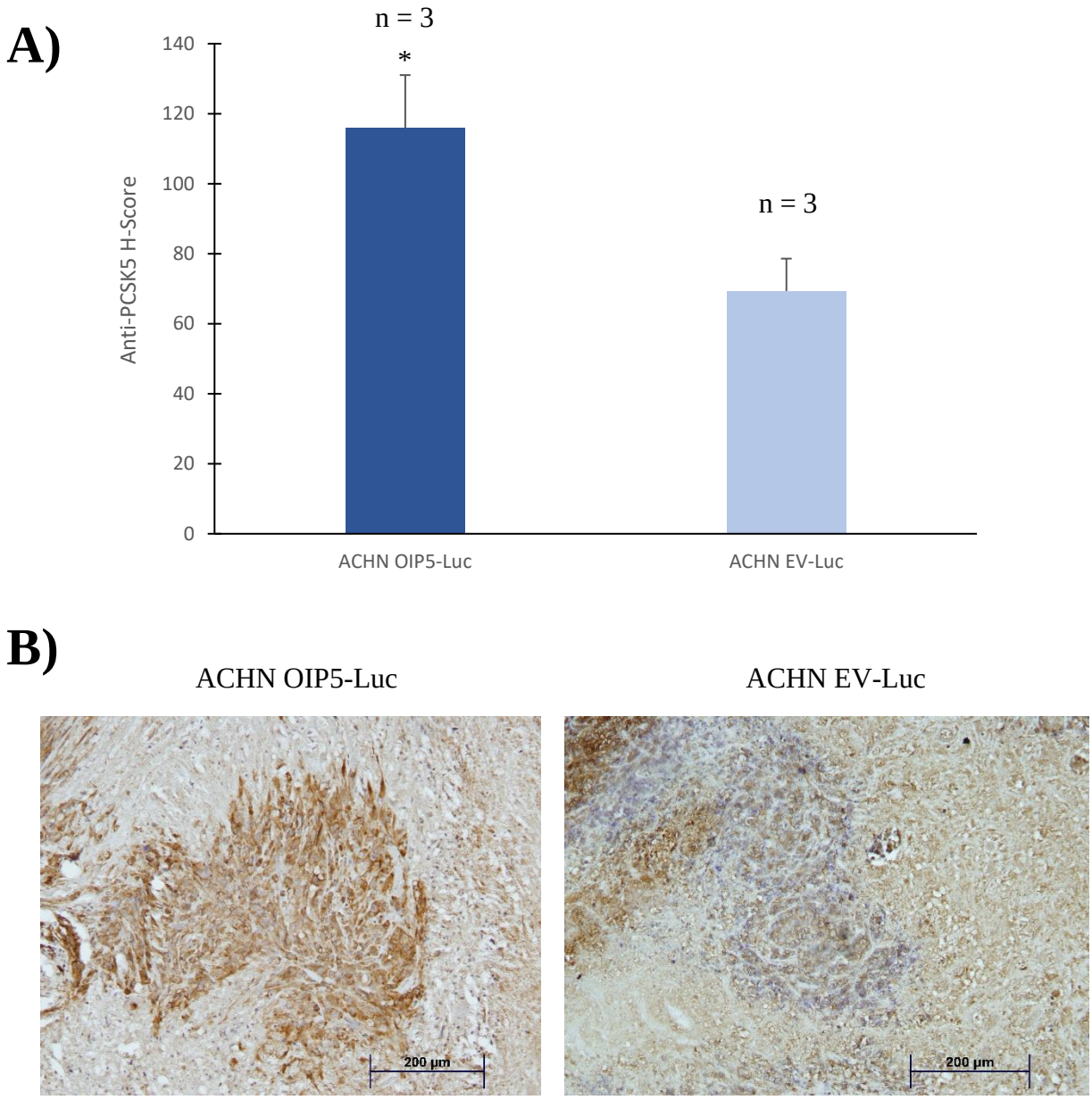

Figure 8. IHC staining and statistical analysis of PCSK5 expression in ACHN OIP5-Luc and ACHN EV-Luc xenograft tumors. **A)** Graph depicting H-score of ACHN OIP5-Luc and ACHN EV-Luc xenograft tumors after staining with anti-PCSK5. Experiment was repeated 3 times (n = 3). Student t-test was used to statistically analyze the results. Data shown is mean + SE. * indicates a significant difference between groups. * indicates $p \leq 0.05$. **B)** Images of anti-PCSK5 IHC staining for ACHN OIP5-Luc and ACHN EV-Luc xenograft tumors.

To further demonstrate an elevation of PCSK5 protein in OIP5 tumors, I have analyzed subcutaneous (s.c.) xenografts produced by ACHN EV and OIP5 cells, which were produced by a previous graduate student Mathilda Chow (Chow et al., 2021). Slides of ACHN OIP5 and ACHN EV xenograft tumors obtained from Chow (2020) were cut and stained with a PCSK5 detection antibody to investigate its expression levels in pRCC tumor tissues with regards to OIP5 overexpression (**Figure 9**). 3 different ACHN OIP5 and ACHN EV xenograft tumors were analyzed. H-score data and statistical analysis show that there is a significant difference in PCSK5 staining intensity between ACHN OIP5 and ACHN EV groups. Collectively, upregulation of PCSK5 by OIP5 is not affected by Luc expression nor by tumors produced by renal capsule transplantation or s.c., further supporting OIP5-mediated PCSK5 upregulation during ACHN cell-derived tumorigenesis.

A)

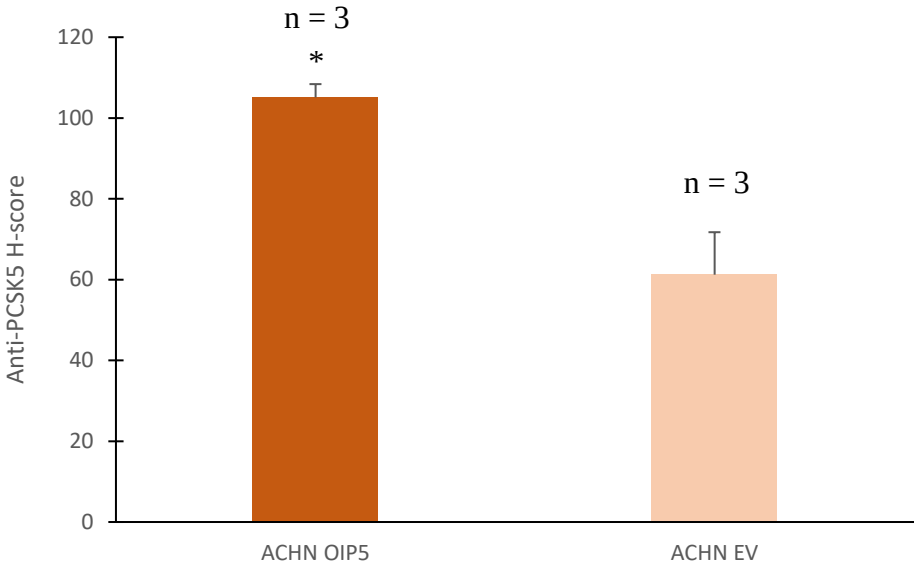

B)

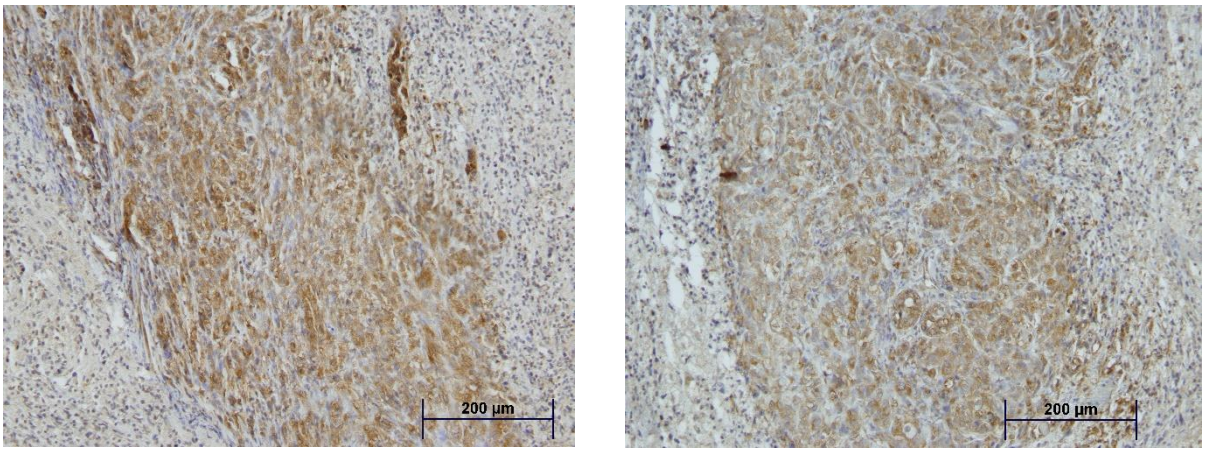

Figure 9. IHC staining and statistical analysis of PCSK5 expression in ACHN OIP5 and ACHN EV xenograft tumors. **A)** Graph depicting H-score of ACHN OIP5 and ACHN EV xenograft tumors after staining with anti-PCSK5. Experiment was repeated 3 times (n = 3). Student t-test was used to statistically analyze the results. Data shown is mean + SE. * indicates a significant difference between groups. * indicates $p \leq 0.05$. **B)** IHC anti-PCSK5 staining for expression in ACHN OIP5 and ACHN EV xenograft tumors.

Upregulation of PCSK5 in ACHN OIP5 xenografts is likely relevant to expression interactions between OIP5 and PCSK5 during pRCC pathogenesis in patients. By taking advantage of publicly available TCGA pRCC gene expression data, we detected a positive correlation between OIP5 and PCSK5 gene expression among 283 tumors (Spearman correlation coefficient 0.25, p=1.53e-05, **Figure 10**). Using the public genomic TCGA data organized by UALCAN (Chandrashekar et al., 2017), PCSK5 expression is significantly increased in stage 3 pRCCs compared to stage 1 tumors (**Figure 11**), indicating an association of PCSK5 expression with pRCC progression. As pRCC severity is an established prognostic biomarker, the association of PCSK5 with pRCC stage advancement implies PCSK5's potential as a prognostic biomarker. This possibility is supported by the significant stratification of pRCC patients' overall survival probability by PCSK5 gene expression; specifically, tumors with high PCSK5 expression are associated with poor overall survival (**Figure 12**). Taken together, my research supports the role of PCSK5 in promoting pRCC tumorigenesis.

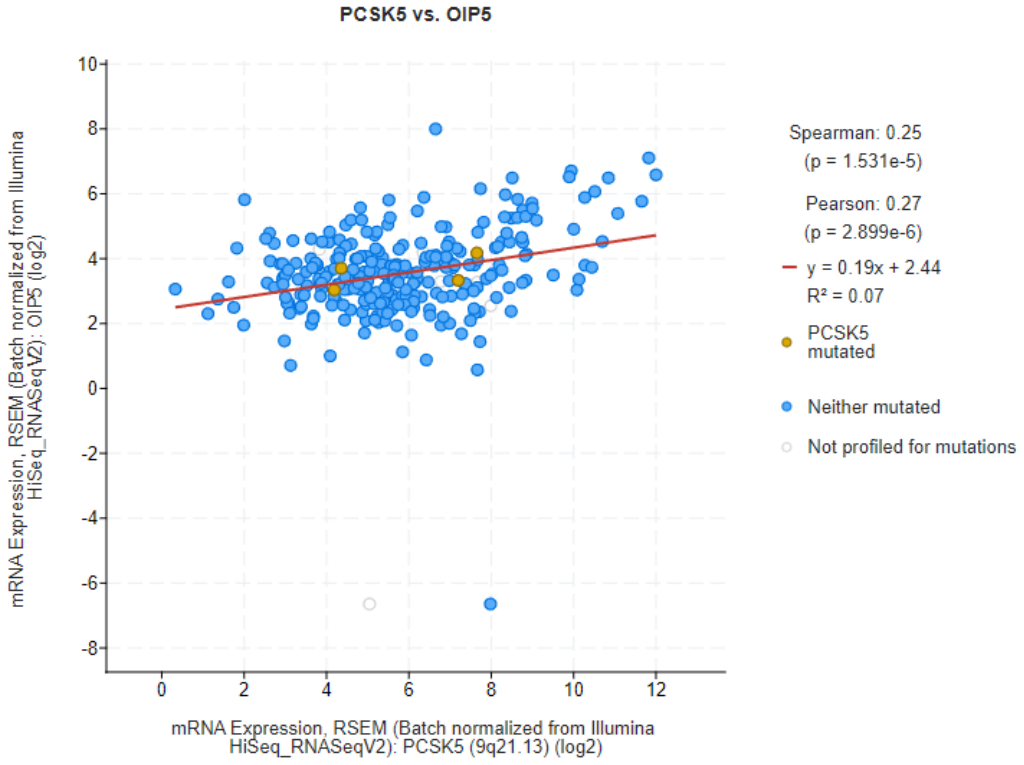

Figure 10. Correlation of PCSK5 mRNA expression levels with OIP5 mRNA expression levels. The figures were generated with data obtained from cBioPotal TCGA PanCancer pRCC dataset. N = 283.

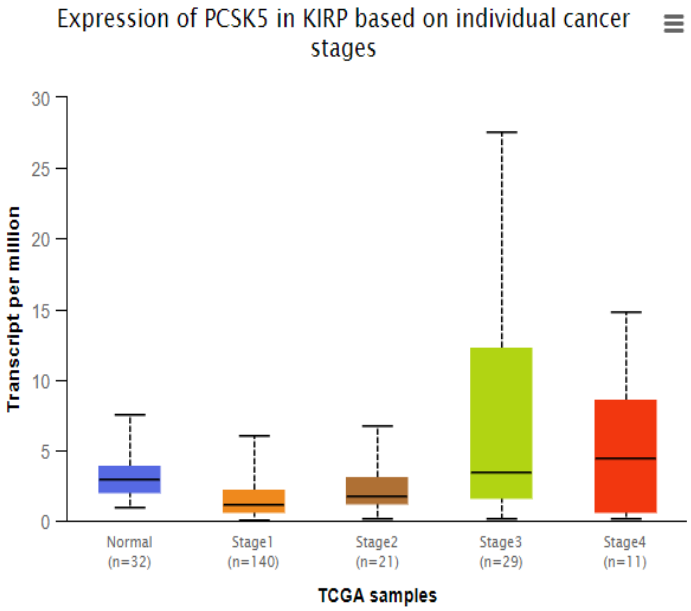

Comparison	Statistical significance
Normal-vs-Stage1	3.823200E-01
Normal-vs-Stage2	2.764800E-01
Normal-vs-Stage3	4.179500E-03
Normal-vs-Stage4	1.553220E-01
Stage1-vs-Stage2	2.429400E-01
Stage1-vs-Stage3	2.858000E-03
Stage1-vs-Stage4	1.420030E-01
Stage2-vs-Stage3	5.852000E-01
Stage2-vs-Stage4	5.127000E-01
Stage3-vs-Stage4	7.453600E-01

Figure 11. Boxplot depicting PCSK5 RNA levels in different stages of pRCC cancer progression. Comparisons between normal vs. stage 3 and stage 1 vs. stage 3 were statistically significant.

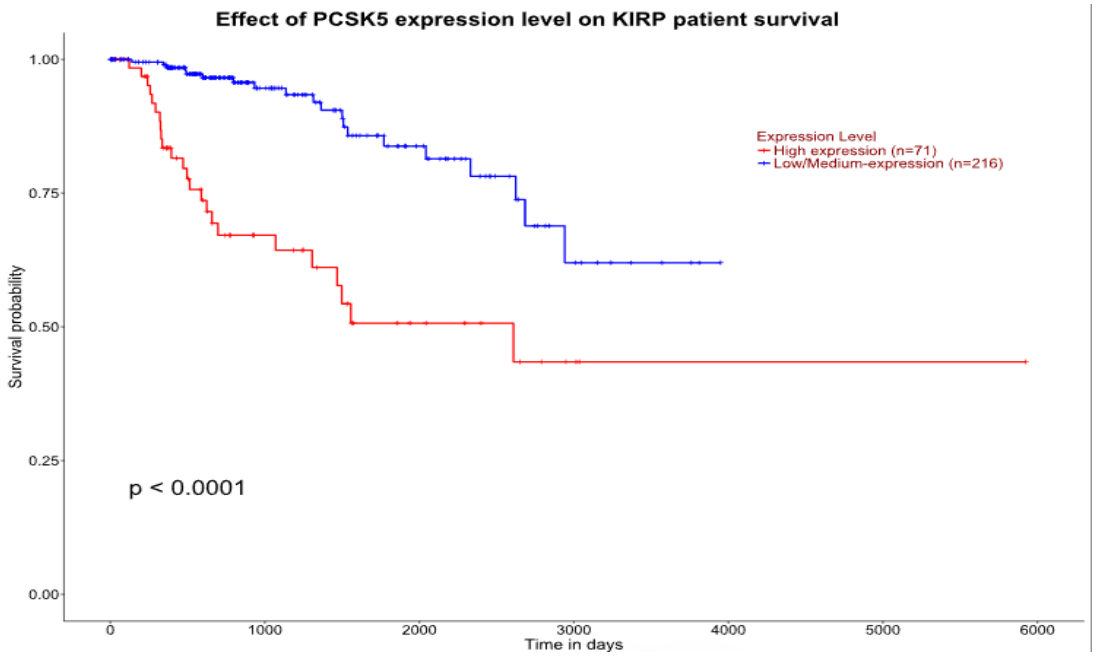

Figure 12. Survival probability of patients in days in relation to PCSK5 expression levels. Graph obtained from UALCAN pRCC dataset analysis.

5. DISCUSSION

RCC accounts for approximately 3% of all human cancers and the incidence rate as well as annual death rate are slowly increasing each year (Chow, 2020; Hsieh et al., 2017; WCRF International, 2022). Metastatic RCC remains lethal, although target therapies including immune checkpoint treatments are able to prolong survival (Lin et al., 2020). Current therapeutic treatments to combat RCC metastasis involve immunotherapies that block immune checkpoints and involve immune checkpoint inhibitors, targeting checkpoint proteins such as PD-1 and PD-L1 (Lin et al., 2020). Despite this in conjunction with targeting growth factors and proteins regulating cell survival, RCC metastasis is commonly shown to resist therapeutic treatments (Lin et al., 2020). Research has shown that targeting proteins and molecular targets involved in the metastatic network could provide a feasible therapeutic solution (Dong et al., 2021). Expression of the RKIP protein, which is a prostate cancer (PC) metastasis suppressor, inhibits PC metastasis, reduces PC cell invasive potential, and causes sensitivity to therapeutic treatment (Dong et al., 2021). Investigating the RCC metastasis network and identifying proteins involved in suppressing metastasis is warranted. Early diagnosis is an effective solution to reducing RCC death in patients. However, as early tumor growth is asymptomatic, diagnosis may often occur when RCC has already progressed to late stages. It is thus critical to advance our understanding on RCC through further investigation and discoveries.

OIP5 as a novel oncogenic factor in pRCC is a recently discovered development (Chow et al., 2021). OIP5 plays an important role during cell replication; it acts in a complex as Mis18β to aid in CENP-A nucleosome localization and kinetochore formation for proper chromosome separation in mitosis. While these essential functions of OIP5 in cell cycle progression support its

involvement in tumorigenesis, this possibility has not been thoroughly investigated. Nonetheless, evidence is emerging. For pRCC, OIP5 was shown to promote ACHN cells to form xenografts in a mouse s.c. model in which PLK1 and PCSK5 were upregulated and inhibition of PLK1 kinase activity reduced OIP5-promoted tumor growth (Chow et al., 2021). These functional studies together with the association of OIP5 upregulation with a significant decrease in overall survival possibility (Chow et al., 2021) strongly support OIP5 facilitating pRCC tumorigenesis via a network action which at least in part involves PLK1 and PCSK5. Nonetheless, this concept needs to be further investigated. For instance, the functional impacts of OIP5 and its network involved in promoting ACHN tumorigenesis obtained using the subcutaneous xenograft model (Chow et al., 2021) may need to be validated using an orthotopic RCC model; the model allows analysis of tumor formation and growth in the kidney environment, which is a more physiologically accurate model compared to the s.c. pRCC model. Another advantage of using the renal capsule orthotopic RCC model is the model being supportive of cancer metastasis. In this regard, I have introduced luciferase into ACHN EV and ACHN OIP5 cells and followed through the course of live tumorigenesis in mice through live imaging of the renal subcapsular space.

Through using this orthotopic model, my research validated the observations obtained using an s.c. tumor model (Chow et al., 2021), i.e. OIP5 enhances pRCC tumorigenesis along with upregulation of both PLK1 and PCSK5. These upregulations were observed at the protein expression level, which was consistent with previously observed upregulations of PLK1 and PCSK5 at mRNA level (Chow et al., 2021).

Metastasis is the major cause of cancer death, contributing to more than 90% of cancer fatalities worldwide (Gu et al., 2020). This is majorly due to loss of apoptotic function (Mehlen,

Puisieux, 2006). RCC metastatic spread occurs in approximately 33% of patients (Flanigan et al., 2003). With metastatic RCC, clinical treatment becomes more difficult and common metastatic sites include the adrenal gland and lungs (Flanigan et al., 2003). Evidence also supports a role of OIP5 in facilitating bladder cancer (Wang et al., 2018). Therefore, it is important to investigate OIP5's role in pRCC metastasis. While our orthotopic model coupled with luciferase in order to monitor cancer metastasis is capable of detecting cancer metastasis (Naito et al., 1987), my research is inconclusive for showing a potential role of OIP5 in pRCC metastasis. At the endpoint, OIP5 did lead to larger two-dimensional tumor volume, indicating the tumors had elevated invasive ability, an ability which is required for cancer metastasis. However, there were little signs indicating metastasis had occurred, as nearby organs where RCC commonly targets for metastasis such as the lungs were found unaffected. The inability to detect distant metastasis could be due to a number of reasons. The sensitivity of the imaging system may not be high enough to detect minor metastasis events; the rapid tumor growth in the nude mice may not give sufficient time for distant metastasis to occur due to the rapidly deteriorating health conditions of the mice as tumor volume increased; also, the lack of an immune component in nude mice might be a factor. My experiment conditions were also not optimized for distant metastasis. For instance, only 3 mice were able to be visualized and investigated for each of the EV and OIP5 groups, which was due to animal loss following surgery. All these factors should be considered in the future when addressing OIP5's function in pRCC metastasis.

Even with the above limitations, my research confirmed OIP5's oncogenic role in pRCC as previously reported (Chow et al., 2021). Of importance, my work not only validated PLK1 and PCSK5 being upregulated by OIP5 but also suggested a functional impact of PCSK5 in pRCC. In

addition to xenografts, I was able to show the clinical relevance of PCSK5 expression in pRCC; PCSK5 expression was increased in advanced stages of pRCC and pRCCs with high PCSK5 expression are associated with poor overall survival. Clearly, PCSK5's oncogenic roles in pRCC require further investigations.

6. FUTURE DIRECTION

The results of this study indicate that OIP5 overexpression promotes cell proliferation and tumorigenesis *in vitro* and *in vivo*. Further investigations are warranted, especially with regards to the dynamics of metastatic potential and tumor growth in different live models. Furthermore, PCSK5's role in the later stages of pRCC progression should also be studied as it may indicate an underlying role in developed tumors and may involve OIP5 as well. These experiments also should eventually be conducted on ccRCC and other RCC subtypes as the different dynamics of each subtype may provide more information on the genes of interest and the underlying mechanisms of RCC as a whole. Lastly, studying the proteins and molecular targets downstream of OIP5 would be beneficial to discover the underlying interactions and mechanisms associated with OIP5's promotion of RCC.

7. REFERENCES

Boussouar, F., Jamshidikia, M., Morozumi, Y., Rousseaux, S., & Khochbin, S. (2013). Malignant genome reprogramming by ATAD2. *Biochimica Et Biophysica Acta (BBA) - GeneRegulatory Mechanisms*, *1829*(10), 1010–1014. https://doi.org/10.1016/j.bbagrm.2013.06.003

Brito, M. B., Goulielmaki, E., Papakonstnti, E. A. (2015) Focus on PTEN regulation. *Front Oncol*, **5**, 166

Cao, H., Mok, A., Miskie, B., & Hegele, R. A. (2001). Single-nucleotide polymorphisms of the proprotein convertase subtilisin/kexin type 5 (PCSK5) gene. *Journal of Human Genetics*, *46*(12), 730–732. https://doi.org/10.1007/s100380170008

Chandrashekar, D. S., Bashel, B., Balasubramanya, S. A., Creighton, C. J., Ponce-Rodriguez, I., Chakravarthi, B. V. S. K., & Varambally, S. (2017). UALCAN: A portal for facilitating tumor subgroup gene expression and survival analyses. *Neoplasia*, *19*(8), 649–658. https://doi.org/10.1016/j.neo.2017.05.002

Chow, M. 2020, 'The Examination of OIP5 Expression In Renal Cell Carcinoma (RCC) andDuring RCC Progression', MSc thesis, McMaster University, Hamilton

Chow, M. J., Gu, Y., He, L., Lin, X., Dong, Y., Mei, W., Kapoor, A., & Tang, D. (2021). Prognostic and therapeutic potential of the OIP5 network in papillary renal cell carcinoma. *Cancers*, *13*(17), 4483. https://doi.org/10.3390/cancers13174483

Dong, Y., Lin, X., Kapoor, A., Gu, Y., Xu, H., Major, P., & Tang, D. (2021). Insights of RKIP-derived suppression of prostate cancer. *Cancers*, *13*(24), 6388. https://doi.org/10.3390/cancers13246388

Flanigan, R. C., Campbell, S. C., Clark, J. I., & Picken, M. M. (2003). Metastatic renal cell carcinoma. *Current Treatment Options in Oncology*, *4*(5), 385–390. https://doi.org/10.1007/s11864-003-0039-2

Gao, Z., Man, X., Li, Z., Bi, J., Liu, X., Li, Z., … Kong, C. (2019). PLK1 promotes proliferation and suppresses apoptosis of renal cell carcinoma cells by phosphorylating MCM3. *Cancer Gene Therapy*, *27*(6), 412–423. https://doi.org/10.1038/s41417-019-0094-x

Golsteyn, R. M., Mundt, K. E., Fry, A. M., & Nigg, E. A. (1995). Cell cycle regulation of the activity and subcellular localization of Plk1, a human protein kinase implicated in mitotic spindle function. *Journal of Cell Biology*, *129*(6), 1617–1628. https://doi.org/10.1083/jcb.129.6.1617

Gong, M., Xu, Y., Dong, W., Guo, G., Ni, W., Wang, Y., … An, R. (2013). Expression of Opa interacting protein 5 (OIP5) is associated with tumor stage and prognosis of clear cell renal cell carcinoma. *Acta Histochemica*, *115*(8), 810–815. https://doi.org/10.1016/j.acthis.2013.03.008

Gray, R. E., Harris, G. T. (2019) Renal Cell Carcinoma: Diagnosis and Management. *Am Fam Physician*, 99, 179-184

Gu, Y., Li, T., Kapoor, A., Major, P., & Tang, D. (2020). Contactin 1: An important and emerging oncogenic protein promoting cancer progression and metastasis. *Genes*, *11*(8), 874. https://doi.org/10.3390/genes11080874

Gutteridge, R. E., Ndiaye, M. A., Liu, X., & Ahmad, N. (2016). PLK1 inhibitors in cancer therapy: From laboratory to clinics. *Molecular Cancer Therapeutics*, *15*(7), 1427–1435. https://doi.org/10.1158/1535-7163.mct-15-0897

Hatzivassiliou, G., Song, K., Yen, I., Brandhuyber, B., Anderson, D., Alvarado, R., Ludlam, M., Stokoe, D., Gloor, S., Vigers, G., et al. (2003) RAF inhibitors prime wild-type RAF to activate the MAPK pathway and enhance growth. *Nature*. **464**, 431-435

Hoac, B., Susan-Resiga, D., Essalmani, R., Marcinkiweicz, E., Seidah, N. G., & McKee, M. D. (2018). Osteopontin as a novel substrate for the proprotein convertase 5/6 (PCSK5) in Bone. *Bone*, *107*, 45–55. https://doi.org/10.1016/j.bone.2017.11.002

Hsieh, J., Purdue, M., Signoretti, S. et al. Renal cell carcinoma. *Nat Rev Dis Primers 3*, 17009 (2017). https://doi-org.libaccess.lib.mcmaster.ca/10.1038/nrdp.2017.9

Hua, L., Zhang, L., Zhang, X., Cui, Z. (2017) PI3K/AKT/mTOR pathway promotes progestin resistance in endometrial cancer cells by inhibition of autophagy. *Onco Targets Ther*. **10**, 2865-2871

Ji, S., Su, X., Zhang, H., Han, Z., Zhao, Y., & Liu, Q. (2018). MicroRNA-372 functions as a tumor suppressor in cell invasion, migration and epithelial-mesenchymal transition by targetingATAD2 in renal cell carcinoma. *Oncology Letters*. https://doi.org/10.3892/ol.2018.9871

Kidney Cancer. Canadian Cancer Survivor Network. (2020). https://survivornet.ca/cancer-type/kidney-cancer/.

Kidney cancer statistics: World cancer research fund international. WCRF International. (2022, April 14). Retrieved August 16, 2022, from https://www.wcrf.org/cancer-trends/kidney-cancer-statistics/

Koinuma, J., Akiyama, H., Fujita, M., Hosokawa, M., Tsuchiya, E., Kondo, S., Nakamura, Y., Daigo, T. (2012) Characterization of an Opa Interacting Protein 5 Involved in Lung and Esophageal Carcinogenesis. *Cancer Sci*. **103**, 577-586

Leal-Esteban, L. C., & Fajas, L. (2020). Cell cycle regulators in cancer cell metabolism. *Biochimica Et Biophysica Acta (BBA) - Molecular Basis of Disease*, *1866*(5), 165715. https://doi.org/10.1016/j.bbadis.2020.165715

Li, H., Zhang, J., Lee, M., Yu, G., Han, X., Kim, D. (2017) OIP5, a target of miR-15b-5p, regulates hepatocellular carcinoma growth and metastasis through the AKT/mTORC1 and β-catenin signaling pathways. *Oncotarget*. **8**, 18129- 18144

Li, L., Zhao, G. D., Shi, Z., Qi, L., Zhou, L., Fu, Z. (2016) The Ras/Raf/MEK/ERK signaling pathway and its role in the occurrence and development of HCC. *Oncol Lett*, **12**, 3045-3050

Li, Y., Xiao, F., Li, W., Hu, P., Xu, R., Li, G., Zhu, C. (2019) Overexpression of Opa interacting protein 5 increases the progression of liver cancer via BMPR2/JUN/CHEK1/RAC1 dysregulation. *Oncol Rep*, **41**, 2075-2088

Lin, X., Kapoor, A., Gu, Y., Chow, M. J., Peng, J., Major, P., & Tang, D. (2020). Construction of a novel multigene panel potently predicting poor prognosis in patients with clear cell renal cell carcinoma. *Cancers*, *12*(11), 3471. https://doi.org/10.3390/cancers12113471

Mancini, M., Righetto, M., & Baggio, G. (2020). Gender-Related Approach to Kidney Cancer Management: Moving Forward. *International Journal of Molecular Sciences*, *21*(9), 3378. https://doi.org/10.3390/ijms21093378

McKinley, K. L., Cheeseman, I. M. (2015) Polo-like kinase 1 licenses CENP-A deposition at centromeres. *Cell*, **158**, 397-411

Mehlen, P., & Puisieux, A. (2006). Metastasis: A question of life or death. *Nature Reviews Cancer*, *6*(6), 449–458. https://doi.org/10.1038/nrc1886

Meyer, H.-A., Tölle, A., Jung, M., Fritzsche, F. R., Haendler, B., Kristiansen, I., … Kristiansen, G. (2009). Identification of Stanniocalcin 2 as Prognostic Marker in Renal Cell Carcinoma. *European Urology*, *55*(3), 669–678. https://doi.org/10.1016/j.eururo.2008.04.001

Muglia, V. F., & Prando, A. (2015). Renal cell carcinoma: histological classification and correlation with imaging findings. *Radiologia Brasileira*, *48*(3), 166–174. https://doi.org/10.1590/0100-3984.2013.1927

Naito, S., Giavazzi, R., Walker, S. M., Itoh, K., Mayo, J., & Fidler, I. J. (1987). Growth and metastatic behavior of human tumor cells implanted into nude and beige nude mice. *Clinical & Experimental Metastasis*, *5*(2), 135–146. https://doi.org/10.1007/bf00058059

Pan, D., Walstein, K., Take, A., Bier, D., Kaiser, N., & Musacchio, A. (2019). Mechanism of centromere recruitment of the CENP-A chaperone HJURP and its implications for centromere licensing. *Nature Communications*, *10*(1). https://doi.org/10.1038/s41467-019-12019-6

Pentakota, S., Zhou, K., Smith, C., Maffini, S., Petrovic, A., Morgan, G. P., Weir, J. R., Vetter, I. R., Musacchio, A., Luger, K. (2017). Decoding the centromeric nucleosome through CENP-N. *ELife*, *6*. https://doi.org/10.7554/elife.33442

Renal Cell Cancer Treatment (PDQ®)–Patient Version. National Cancer Institute. (2022). https://www.cancer.gov/types/kidney/patient/kidney-treatment-pdq.

Sanchez-Gastaldo, A., Kempf., E., Alba, A. G., Duran, I. (2017) Systemic treatment of renal cell cancer: A comprehensive review. *Can Treat Rev*. **60**, 77-89

Seidah N.G., Chretien M., (1999) Proprotein and prohormone convertases: a family of subtilases generating diverse bioactive polypeptides. *Brain Res*, *848*, 45–62

Wang, D., Chen, Z., Lin, F., Wang, Z., Gao, Q., Xie, H., Xiao, H., Zhou, Y., Zhang, F., Ma, Y., Mei, H., Cai, Z., Liu, Y., & Huang, W. (2018). OIP5 promotes growth, metastasis and chemoresistance to cisplatin in bladder cancer cells. *Journal of Cancer*, *9*(24), 4684–4695. https://doi.org/10.7150/jca.27381

Yamada, Y., Nohata, N., Uchida, A., Kato, M., Arai, T., Moriya, S., … Seki, N. (2020, February 22). *Replisome genes regulation by antitumor miR-101-5p in clear cell renal cell carcinoma*. Wiley Online Library. https://onlinelibrary.wiley.com/doi/full/10.1111/cas.14327.